Quantitative analysis of chaotic synchronization by means of coherence

A. Shabunin* and V. Astakhov
Radiophysics and Nonlinear Dynamics Department of the Saratov State University, Astrakhanskaya 83, Saratov, Russia

J. Kurths
Nonlinear Dynamics Laboratory of the Potsdam University, Neuen Palace 19, Potsdam, Germany
(Received 21 February 2005; published 27 July 2005)

We use an index of chaotic synchronization based on the averaged coherence function for the quantitative analysis of the process of the complete synchronization loss in unidirectionally coupled oscillators and maps. We demonstrate that this value manifests different stages of the synchronization breaking. It is invariant to time delay and insensitive to small noise and distortions, which can influence the accessible signals at measurements. Peculiarities of the synchronization destruction in maps and oscillators are investigated.

DOI: 10.1103/PhysRevE.72.016218 PACS number(s): 05.45.Xt

I. INTRODUCTION

Synchronization of oscillations traditionally attracts a great interest of researchers because this subject is of fundamental importance for the understanding of nature and for many applications. Since its discovery, synchronization of chaotic oscillations remains in the focus of investigations. Coupled chaotic oscillators demonstrate different types of interdependent behavior which are usually called "chaotic synchronization": from complete coincidence of oscillators trajectories [complete synchronization (CS) [1–3]] till frequency and phase lockings [frequency synchronization (FS) [4], phase synchronization (PS) [5]]. Signals generated by oscillators can demonstrate quite complex functional interdependence [generalized synchronization (GS) [6]] alongside with possible time delaying [lag-synchronization (LS) [7]]. In the framework of these definitions one can distinguish perfect and imperfect synchronization. This variety of complex synchronizations calls for general methods for both quantification and identification of different types of chaotic synchronization which can be applied to experimental data and which enable to compare different stages of synchronous behavior. An appropriate quantitative characteristic for measuring interdependency between signals from coupled oscillators should satisfy the following requirements.

(1) It must be universal for being applied to different types of synchronous behavior. This is essential because different synchronization phenomena are not independent from each other. They can represent different stages of the single process of mutual adjustment of coupled oscillators behavior.

(2) It must represent a normalized quantity in some fixed interval. It is convenient to choose 0 for totally unsynchronized oscillations till 1 for fully synchronized ones.

(3) It must have a clear physical meaning to interpret the obtained results.

(4) It must be independent of a particular type of equations of a dynamical system, thus, being calculated from the time series generated by subsystems.

(5) It must be robust to small noise and distortions.

Attempts to find such a universal characteristic, having been proposed recently, are based mostly on measuring mutual information [8,9], index of nonlinear interdependencies [8,10–13] or recurrent plots approach [14]. The large number of proposed algorithms and their modifications discussed in the literature evidence that finding a good synchronization measure remains a nontrivial task. In Refs. [15,16] we proposed a synchronization index, that is based on other principles: measuring averaged coherence between oscillations, thus using the frequency domain instead of the time domain. In this work we use this index for the investigation of the process of complete synchronization breaking in coupled discrete maps and coupled Rossler oscillators. We also test it under noise influence and distortions of the generated signals. This paper is organized as follows. Section II contains a brief description of the approach for measuring chaotic synchronization. In Sec. III we consider the process of successive destroying of complete chaotic synchronization in two master-slave coupled logistic maps. We analyze the behavior of the synchronization index with coupling from fully synchronized to totally unsynchronized oscillations for different types of chaotic attractors: a one-band attractor with a smooth power spectrum and a two-band one with a spectrum containing discrete peaks. We check the sensitivity of the measured dependence with respect to additive noise and distortions of the considered data. In Sec. IV we carry out a similar research of an oscillatory system: two unidirectionally coupled Rossler oscillators in the regimes of spiral and funnel attractors. We explore the behavior of the coherence function and show that the full coherence on the basic frequency and its harmonics coincides with the phenomenon of phase synchronization, while its partial coherence leads to imperfect phase synchronization. The conclusion contains summary and discussion of the obtained results.

II. INDEX OF SYNCHRONIZATION BASED ON COHERENCE

The main idea of the method is the following. We consider two scalar chaotic signals $x(t)$ and $y(t)$ from two

*Electronic address: alexey@chaos.ssu.runnet.ru

coupled oscillators. In terms of frequencies a time-series of each signal can be represented by its Fourier image $F_x(\omega)$ or $F_y(\omega)$:

$$F_{x,y}(\omega) = |F_{x,y}(\omega)|\exp[j\theta_{x,y}(\omega)] = \int_{-\infty}^{\infty} x(t)[y(t)]\exp(-j\omega t)dt.$$

Here $\theta_{x,y}(\omega)$ are the Fourier-phases of the signals at the frequency ω. From the Fourier images we can calculate the power spectra of the signals

$$P_{x,y}(\omega) = \langle F_{x,y}(\omega)F^*_{x,y}(\omega)\rangle$$

and their cross spectrum

$$C_{xy}(\omega) = \langle F_x(\omega)F^*_y(\omega)\rangle,$$

where $\langle\ \rangle$ denote averaging on ensembles or on time (we suppose the signals to represent ergodic processes). These characteristics describe the processes and their interdependence in terms of frequencies. Normalizing the cross spectrum to the power spectra

$$\sigma_{xy}(\omega) = \left| \frac{C_{xy}(\omega)}{\sqrt{P_x(\omega)P_y(\omega)}} \right|,$$

we obtain the coherence function $\sigma(\omega)$ which characterizes the phase coherence between oscillations on the frequency ω: $\sigma(\omega)=1$ for the frequencies at which differences between the Fourier-phase remain constant ($\theta_x(\omega)-\theta_y(\omega)=$const) and $\sigma(\omega)\to 0$ for those frequencies at which the phases are totally independent and hence, their differences $\theta_x(\omega)-\theta_y(\omega)$ take random values uniformly distributed in $[-\pi;\pi]$ [the strict equality $\sigma(\omega)=0$ takes place if the number of data points approach infinity].

Describing the interdependence between oscillations in terms of frequency, the coherence function represents a very useful tool for signal analysis. However, it does not give a quantitative measure as some normalized value, which would characterize the level of interdependencies between signals for all frequencies simultaneously. To get such a value, we must average the coherence function over all frequencies taking into account the contribution of every harmonic to the power of the signals

$$\bar{\sigma}_{xy} = \int_0^{\infty} h(\omega)\sigma_{xy}(\omega)d\omega, \tag{1}$$

where $h(\omega)=P_x(\omega)+P_y(\omega)$ is a weight function representing the power density on the frequency ω. This defined characteristic $\bar{\sigma}_{xy}$ can take a positive value between 0 and the total power of the considered signals. Then, normalizing the averaged coherence (1) to the power, we get a value fixed in the interval [0;1]. Thus, we define the level of synchrony S between the signals x and y as the averaged coherence magnitude divided by the whole power of both signals:

$$S_{xy} = \frac{\bar{\sigma}_{xy}}{\int_0^{\infty}[P_x(\omega)+P_y(\omega)]d\omega}. \tag{2}$$

This value can be interpreted as the ratio of the power of coherent motions to the total power of the considered signals x and y. It ranges from $S=0$ for signals which are incoherent at all frequencies $[\sigma(\omega)\equiv 0]$ to $S=1$ for totally coherent signals $[\sigma(\omega)\equiv 1]$.

The index of synchronization defined by Eq. (2) can be easily modified if we are interested in interdependence of oscillations in some particular interval $\omega_1 \leqslant \omega \leqslant \omega_2$. In this case we can just change the limits of the integrals as

$$\hat{S}_{xy}(\omega_1,\omega_2) = \frac{\int_{\omega_1}^{\omega_2} h(\omega)\sigma_{xy}(\omega)d\omega}{\int_{\omega_1}^{\omega_2}[P_x(\omega)+P_y(\omega)]d\omega}. \tag{3}$$

This quantity enables a selective evaluation of synchronization index separately for "fast" and "slow" motions.

Numerical calculations of the index (2) are based on well-defined algorithms of spectral analysis (see for example Ref. [17]), which have highly developed theoretical backgrounds. The obtained results are sufficiently stable with respect to the choice of the parameters of the numerical scheme. The precision of the calculation mostly depends on the quality of the statistical data processing: the relative error of the calculated index depends on the number of data points N approximately as $1/\sqrt{N}$.

III. DESTRUCTION OF COMPLETE CHAOTIC SYNCHRONIZATION IN A SYSTEM WITH DISCRETE TIME

Now we show how the proposed synchronization index can be used for the analysis of process of complete chaotic synchronization breaking in two discrete maps. We study a system of two coupled logistic maps in the form

$$x(n+1) = f(x(n)),$$

$$y(n+1) = f(y(n) + \gamma[x(n) - y(n)]), \tag{4}$$

where $f(x)=\alpha x(1-x)$ is the logistic map which represents a typical example of a system with a cascade of period-doubling bifurcations. The parameter α determines the character of motions in a single map, while $0 \leqslant \gamma < 1$ is the coupling coefficient.

Two coupled logistic maps are typically used for investigating complete chaotic synchronization. They demonstrate a wide spectrum of phenomena, which accompany the process of synchronization breaking, such as bubbling of an attractor [18,19], riddled basins [20] and developed phase multistability. The evolution of these phenomena and their bifurcational mechanisms have been studied in a number of works [21–23]. In the present work we consider a master-slave unidirectional type of coupling, because it leads to a simpler

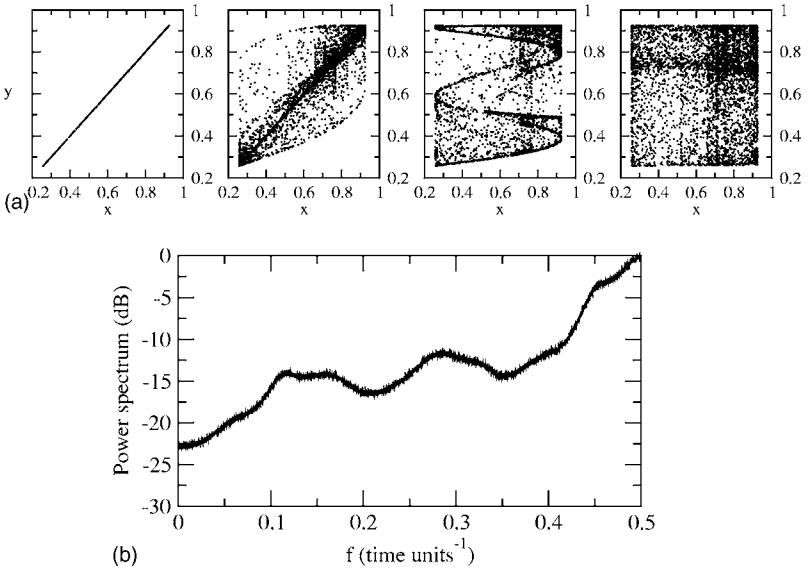

FIG. 1. (a) Phase portraits of system (4) at $\alpha=3.7$ for successively decreased coupling: $\gamma=0.32$, $\gamma=0.29$, $\gamma=0.1$, $\gamma=0.005$ (from left to right) and (b) a power spectrum of the oscillations calculated from the signal $x(n)$.

structure of the phase space compared to the typically used diffusive or linear couplings and it allows one to investigate the phenomenon of synchronization breaking in a wide range of γ. The dynamics of system (4) was in detail described in Ref. [24]. It demonstrates the phenomenon of complete chaotic synchronization at sufficiently large coupling. Decreasing of the coupling firstly leads to weak synchronization, when synchronous oscillations remain only in the system without noise, then to a break of the synchronization through a blowout bifurcation with the appearance of bubbling of the attractor and, at very small coupling, to totally unsynchronized oscillations. These typical qualitative changes taking place with decreasing γ are depicted in Fig. 1(a) for a one-band chaotic attractor with a smooth power spectrum [Fig. 1(b)].

Let us consider the process of synchronization breaking in more detail. The stability properties of regular or chaotic oscillations are characterized by Lyapunov exponents which for the system under study have the following form:

$$\Lambda_\tau = \ln \alpha + \lim_{N\to\infty} \frac{1}{N} \sum_{i=1}^{N} \ln|1 - 2x(i)|, \tag{5}$$

$$\Lambda_\perp = \ln \alpha + \lim_{N\to\infty} \frac{1}{N} \sum_{i=1}^{N} \ln|1 - 2y(i) - 2\gamma[x(i) - y(i)]|, \tag{6}$$

where $x(i)$ and $y(i)$ are the coordinates of the phase points belonging to the attractor. When the oscillations are synchronous, the eigenvector of the first exponent (5) directs tangentially to the symmetric subspace $(x=y)$ and, therefore, it is usually called a "tangent Lyapunov exponent." The tangent exponent determines the stability properties of the attractor inside the symmetric subspace to synchronous disturbances. Its sign determines the character of the oscillations: they are periodic for the negative exponent and chaotic for the positive one. The eigenvector of the next exponent (6) directs transversally to the symmetric subspace and it is called a "transversal Lyapunov exponent." For synchronous oscillations it can be written in the form

$$\Lambda_\perp^s = \Lambda_\tau + \ln|1 - \gamma|, \tag{7}$$

where the index s stresses that this form of the exponent relates to a limit set located inside the symmetric subspace. The sign of the exponent $\Lambda_\perp^s$ determines the transversal stability of synchronous oscillations. If it is negative, the synchronous oscillations are transversally stable and, hence, they are realized in experiments. If it is positive, the synchronous oscillations are transversally unstable and they are not realized. A change of the sign of the transversal exponent $\Lambda_\perp^s$ leads to the "blowout bifurcation" at which the synchronous chaotic attractor transforms to a "chaotic saddle." As it follows from Eq. (7), the transversal exponent $\Lambda_\perp^s$ is smaller than the tangent exponent. Hence, it is negative for any regular synchronous oscillations, while in the case of chaotic oscillations it can be both positive or negative depending on the coupling. For the chosen $\alpha=3.7$ dependences of the Lyapunov exponents on γ are depicted in Fig. 2. Two solid lines relate to two Lyapunov exponents: Λ_τ and $\Lambda_\perp$, respectively, while the transversal exponent for synchronous mo-

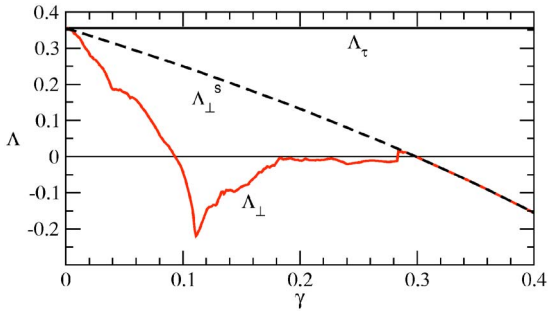

FIG. 2. (Color online) Dependence of the Lyapunov exponents on the coupling at $\alpha=3.7$. The black horizontal line depicts the tangent Lyapunov exponent Λ_τ, while the red solid curve and the dashed curve depict the transversal exponent $\Lambda_\perp$ and the transversal exponent for the synchronous oscillations $\Lambda_\perp^s$, respectively.

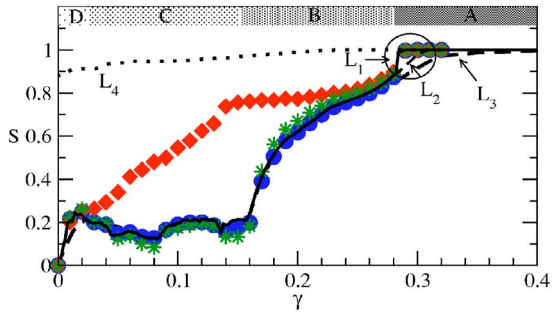

FIG. 3. (Color online) Dependence of the synchronization index S on the coupling strength in the regime of developed chaos ($\alpha=3.7$): L_1 for the noise-free system (4), L_2 for noisy system (8) with $a=10^{-5}$ and L_3 with $a=10^{-2}$. Symbols mark the dependence from the distorted signals u and v: $*$: linear amplification ($u=x$, $v=10y$); ○: weak distortion ($u=x$, $v=y-0.5y^2+0.6y^3$); ◇: strong distortion ($u=x$, $y-0.7y^3$). Dotted line L_4 depicts dependence of S in the regime of two-band chaotic attractor ($\alpha=3.65$).

tions $\Lambda_\perp^s$ is depicted by a dashed curve. While $\gamma>0.298$ the transversal Lyapunov exponent remains negative and, hence, we observe a regime of chaotic synchronization. However, beginning with $\gamma\simeq0.32$ the regime of synchronization becomes "weak," that means that the presence of small noise induces the bubbling process, when most of the time a trajectory remains almost synchronous, but occasionally leaves a neighborhood of the symmetric subspace. Thus, in the regime of weak synchronization the oscillations remain synchronous only in the noise-free case. The value $\gamma=0.298$ is the point of blowout bifurcation after which the synchronous motions become transversally unstable. However, in practice the experimentally observed point of the bifurcation locates slightly further on coupling, near the value $\gamma\simeq0.29$, that can be seen from the coincidence of the curves $\Lambda_\perp$ and $\Lambda_\perp^s$ until this value. After this bifurcation the bubbling behavior is observed both in noisy and noise-free systems. A further decreasing of the coupling leads to developing of the bubbling process, at which bursts apart from the symmetric subspace take place more and more often, while the transversal Lyapunov exponent $\Lambda_\perp$ remains almost constant. Then, at the coupling $\gamma<0.17$ the bubbling development is changed by some structuring inside the chaotic attractor [see Fig. 1(a), $\gamma=0.1$]. At last, at very small coupling we see a totally unsynchronized behavior (Fig. 1, $\gamma=0.005$).

Now, we analyze this process of chaotic synchronization destruction from the point of view of the index of synchronization S (2). Its dependence on the coupling is depicted in Fig. 3 by the solid line L_1. It can be divided into four distinctive parts.

(A) A horizontal line $S=1$ for rather strong coupling, approximately up to $\gamma\simeq0.29$, which relates to the region of complete chaotic synchronization, when $x(n)=y(n)$. In this region the transversal Lyapunov exponent $\Lambda_\perp^s$ is negative (Fig. 2).

(B) A region of monotonic decrease of the synchronization index from $S=1$ till $S\simeq0.2$, which relates to developing the bubbling process. It begins with a sharp fall of the synchronization index from $S=1$ till $S\simeq0.85$ at the blowout bifurcation, after the transversal Lyapunov exponent has crossed zero. Then, the further decreasing of S takes place more gradually. In this region the second Lyapunov exponent $\Lambda_\perp$ oscillates near zero, while the transversal exponent for synchronous oscillations $\Lambda_\perp^s$ is positive (see Fig. 2).

(C) After $\gamma\simeq0.17$ and till very weak coupling $\gamma\simeq0.01$ there is a region where the index of synchronization remains almost constant $S\simeq0.2$. It correlates with some intrinsic rebuilding observed inside the chaotic attractor [Fig. 1(a) at $\gamma=0.1$], which is accompanied by both decreasing and then increasing branches of the second Lyapunov exponent $\Lambda_\perp$.

(D) At last, when $\gamma<0.01$ we observe a rapid decrease of S to zero at zero coupling which is not accompanied by any qualitative change in the behavior of the Lyapunov exponents. The phase portrait of the oscillations looks like the "black square" [Fig. 1(a) at $\gamma=0.005$].

Thus the obtained dependence manifests different stages of the process of chaotic synchronization destruction: from complete synchronization to totally unsynchronized behavior. It is exactly equal to 1 for the perfect synchronization and tends to 0 for uncoupled maps. Different parts of the characteristic are in correlation with the behavior of the Lyapunov exponents, except the region of very small γ.

The considered system of coupled identical maps is a too idealized model for real oscillators. Experimental data usually contain external noise as well as they can be distorted and delayed in the communication channel between the explored object and the measuring devices. Typically, instead of the original time series $x(t)$ we deal with some observable data $G(x(t-\tau))$, where G is a function, which describes a possible distortion and a time-delay of the signal in the communication channel. Hence, the sensitivity to external noise and to different linear or nonlinear distortions and time delays is a very important property for measurements of any dynamical characteristics. This is especially important in the case of biological experiments when we often have no possibility to analyze the original signals generated by investigated objects, while the accessible data can heavily differ from them.

After showing the specificity, we now check the sensitivity of the proposed index S to the mentioned above data modification. To take into account the influence of additive noise and possible distortions in the communication channel, we modify system (4) in the following way:

$$x(n+1)=f(x(n))+a\xi_1(n),$$

$$y(n+1)=f(y(n)+\gamma[x(n)-y(n)])+a\xi_2(n),$$

$$u(n)=G_1(x(n-n_1)),$$

$$v(n)=G_2(y(n-n_2)), \tag{8}$$

where $a\xi_{1,2}(n)$ are two independent sources of noise with uniform distributions and equal amplitudes a, while the analyzed signals $u(n)$ and $v(n)$ represent copies of the original signals $x(n)$ and $y(n)$ transformed according to some deterministic rules G_1 and G_2 and delayed to the time intervals n_1 and n_2. In our investigations we tested separately the sensi-

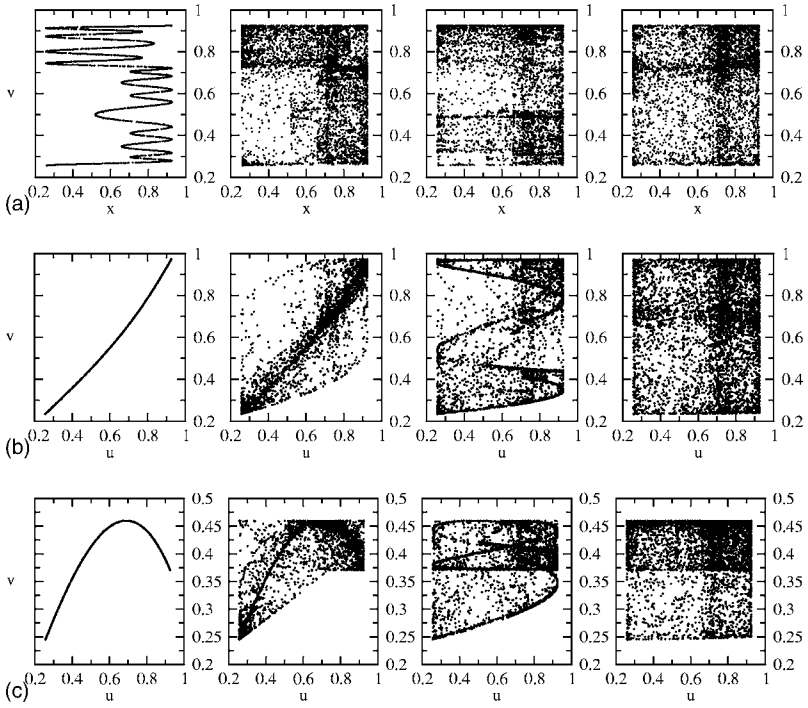

FIG. 4. Phase portraits of the one-band attractor at $\alpha=3.7$ for successively decreased coupling: $\gamma=0.32$, $\gamma=0.29$, $\gamma=0.1$, and $\gamma=0.005$ (from left to right) built from the distorted signals. (a) Linear filtering with time delay: $u(n)=x(n)$, $v(n)=y(n-7)$; (b) weak nonlinear distortion: $u=x$, $v=y-0.5y^2+0.6y^3$; (c) strong nonlinear distortion: $u=x$, $v=y-0.7y^3$.

tivity to noise influence and to distortion and delay of the signals.

(1) Sensitivity to additive noise: This case relates to Eq. (8) with $G_1(x)=x$, $n_1=0$, $G_2(y)=y$, $n_2=0$. Varying the amplitude of the noise from very small: $a=10^{-5}$ [the line L_2 in Fig. 3] till sufficiently large: $a=10^{-2}$ [the line L_3 in Fig. 3] values we find that the noise weakly influences the value S except the region of weak synchronization (it is marked by a circle). If the amplitude of the noise is extremely small, the marked region is the only one where the noisy and the noise-free cases can be distinguished. The sensitivity of the value S to noise in the marked interval of coupling is an evident consequence of the sensitivity of the system behavior to noise in the regime of weak synchronization. If the intensity of noise is not so small, the index of synchronization is slightly changed in the whole interval of coupling [see curve L_3 in Fig. 3].

(2) Sensitivity to delay of the signals: This relates to $G_1(x)=x(n-n_1)$, and $G_2(y)=y(n-n_2)$, $a=0$. The system (8) can be rewritten in the form

$$u(n+1)=f(u(n)),$$

$$v(n+1)=f(v(n)+\gamma[u(n-\Delta n)-v(n)]), \tag{9}$$

where $\Delta n=n_2-n_1$. Complete synchronization in the original system entails lag synchronization in the modified one if $\Delta n<0$ or anticipated synchronization [25] if $\Delta n>0$. As it follows from its definition (2), the synchronization index S is invariant to the time delay of the signals. Indeed, since Fourier transformations are invariant to this data modification up to constant phase shifts,

$$F_u=F_x\exp(-j\omega n_1),$$

$$F_v=F_y\exp(-j\omega n_2),$$

both the coherence function and the power spectra remain the same for the delayed signals: $\sigma_{uv}=\sigma_{xy}$, $P_{u,v}=P_{x,y}$, and, consequently,

$$S_{uv}=S_{xy}. \tag{10}$$

Thus the index of synchronization calculated from both system (4) and system (9) take equal values at the same coupling. The shape of the phase portrait built from a delayed signal can be very complex [this is seen in Fig. 4(a) for $n_1=0$ and $n_2=7$] and does not allow to identify the imperfect synchronization visually. For example, phase portraits for both $\gamma=0.29$ and $\gamma=0.005$ look very similar, though the first case relates to almost synchronous oscillations ($S=0.9996$), while the last case to practically unsynchronized ones ($S=0.102$). Nevertheless, the invariance of the value S to a time delay allows to measure the synchronization index both for complete and lag types of synchronization.

(3) Sensitivity to distortions of the signals: $u(n)=G_1(x(n))$, $v(n)=G_2(y(n))$. If both inverse functions G_1^{-1} and G_2^{-1} are single valued, Eqs. (4) can be rewritten as

$$u(n+1)=g(u(n)),$$

$$v(n+1)=h(v(n),u(n),\gamma), \tag{11}$$

where $g(u)=G_1(f(G_1^{-1}(u)))$, $h(v,u,\gamma)=G_2(f(G_2^{-1}(v)+\gamma[G_1^{-1}(u)-G_2^{-1}(v)]))$. The complete synchronization in the original system (4) entails generalized synchronization $u(n)=G_1(G_2^{-1}(v(n)))$ in the modified one (11). If the inverse functions have several branches of values, we can not rewrite the system in the new variables because of the loss of information in the communication channel which does not allow to

restore the original signals from the observed data. Hence, in this case the distortions in the communication channel can not be considered as a manifestation of generalized synchronization of chaos in the system with the new variables.

Let us consider first the most simple case of signals distortion: linear distortion (amplification in the communicational channels): $u=Ax$, $v=By$. Since the coherence function is invariant to linear transformations of the signals, the index of synchronization S can be written as

$$S_{uv} = \frac{\int_0^\infty \sigma_{xy}(\omega)[A^2 P_x(\omega) + B^2 P_y(\omega)]d\omega}{\int_0^\infty [A^2 P_x(\omega) + B^2 P_y(\omega)]d\omega}. \qquad (12)$$

The value is seen to remain unchanged if $A=B$, that means that the signals are amplified equally in both channels, or if $P_x=P_y$. The last case can take place, for example, for identical oscillators with symmetric coupling. Typically, oscillating regimes in the interacting oscillators and, hence, their power spectra, do not differ heavily from each other. Consequently, the value S calculated from the amplified signals will be very close to those from the original ones. This case is realized for the system under study. For example, the results for $A=1$ and $B=10$, when one of the signals is changed by one order of its magnitude, the difference between values S_{xy} and S_{uv} is sufficiently small in the whole interval of coupling. The last case can be seen in Fig. 3, where the index from the amplified signal is depicted with symbols "$*$".

If the distortions are nonlinear, both the coherence function and the power spectrum will be changed. To check their influence on the behavior of the synchronization index, we carried out numerical simulations for two different kinds of distortions: (i) a weak nonlinear distortion $[G_1(x)=x,\ G_2(y)=y-0.5y^2+0.6y^3]$ when the inverse function $G_2(y)$ remains single-valued in the considered interval of y [see. Fig. 4(b)], and (ii) a sufficiently large distortion $[G_1(x)=x,\ G_2(y)=y-0.7y^3]$ with two branches of the $G_2^{-1}(y)$ function [see Fig. 4(c)]. The results of the simulations are depicted in Fig. 3 with symbols "○" and "◇", respectively. It is seen that the results for the slightly distorted signal and for the original ones practically coincide. Since in this case the modified system (11) demonstrates the generalized synchronization, the index S can be applied to this type of synchronous behavior. If the distortion is large, the coincidence exists only in the region of full synchronization and at very small coupling, when synchronization is almost absent. In other regions we observe only a qualitative correspondence between the dependencies.

Thus our analysis and investigations have shown that the proposed characteristic weakly depends on both small noise and small nonlinear distortions, and does not depend on the delay of the signals in the communication channel. If the distortions in the channel are strong, the index of synchronization allows to distinguish cases of full synchronization as well as totally unsynchronized behavior.

So far we analyzed a developed chaotic behavior, for which the correspondent power spectrum is smooth and the

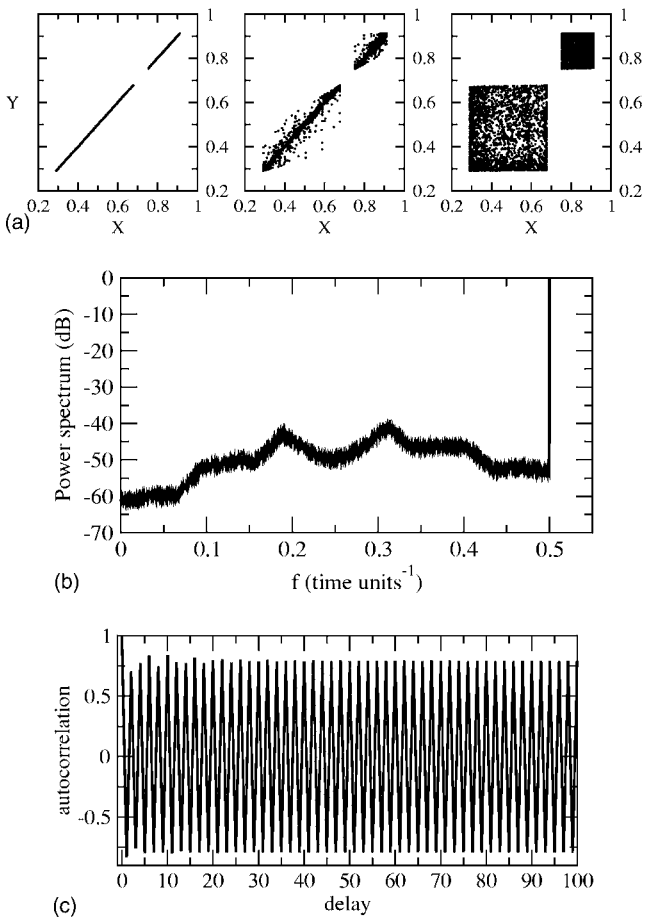

FIG. 5. (a) Phase portraits for coupling $\gamma=0.25$, $\gamma=0.23$, and $\gamma=0.005$ (from left to right), (b) power spectrum, and (c) autocorrelation function of the two-band chaotic attractor ($\alpha=3.65$).

autocorrelation function decays to zero. Next, we study a case, when chaotic behavior contains a periodic component, i.e., multiband chaotic attractors. We consider peculiarities of the complete synchronization breaking in such regimes. For this purpose we choose $\alpha=3.65$ which corresponds to a two-band chaotic attractor [Fig. 5(a)] whose power spectrum contains a δ peak at the frequency $f=0.5$. The process of synchronization breaking goes through the same stages as for the one-band attractor [see Fig. 5(a)]. Changing the coupling coefficient from $\gamma \simeq 0.25$ till $\gamma=0$, we observe first full synchronization, then a transition through the blowout bifurcation and a development of the bubbling process to unsynchronized oscillations at zero coupling. The correspondent dependence of the synchronization index is depicted in Fig. 3 with the dotted curve (line L_4). Contrary to the case of the one-band attractor, it decreases very slow and finally reaches value $S=0.88$ at zero coupling. Hence, the chaotic synchronization in coupled maps has no threshold on coupling in a regime of coherent chaos. This result is not unexpected. Indeed, the presence of the δ peak in the power spectrum evidences that chaotic oscillations contain a periodic component, which manifests itself in the nondecaying character of the autocorrelation function [Fig. 5(c)]. In the absence of phase diffusion, which cannot exist in a discrete time system, the periodic oscillations with equal periods have full coher-

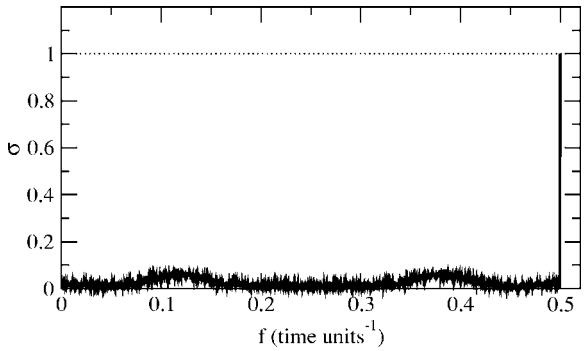

FIG. 6. The coherence function for system (4) in the regime of two-band chaos. $\alpha=3.65$; $\gamma=0$.

ence at the frequency of the periodic component, as seen from their coherent function dependence (Fig. 6). This peculiarity of the synchronization behavior at zero coupling relates to discrete maps. The behavior of the synchronization index for full-scale oscillators described by ordinary differential equations is different.

IV. DESTRUCTION OF COMPLETE CHAOTIC SYNCHRONIZATION IN COUPLED OSCILLATORS

In this section we analyze the process of chaotic synchronization loss in coupled oscillators with continuous time. The used model consists of unidirectionally coupled Rossler oscillators:

$$\dot{x}_1 = -\omega y_1 - z_1,$$

$$\dot{y}_1 = \omega x_1 + a y_1,$$

$$\dot{z}_1 = b + z_1(x_1 - c),$$

$$\dot{x}_2 = -(\omega + \Delta) y_2 - z_2 + \gamma(x_1 - x_2),$$

$$\dot{y}_2 = (\omega + \Delta) x_2 + a y_2,$$

$$\dot{z}_2 = b + z_2(x_2 - c), \tag{13}$$

where the parameters a,b are fixed: $a=0.2$, $b=0.2$, the frequency $\omega=1.0$, Δ characterizes the mismatch between both subsystems. Depending on c, the single oscillator demonstrates periodic oscillations, a cascade of period-doubling bifurcations, many-band and one-band spiral chaotic attractors or a funnel attractor. Without mismatch ($\Delta=0$) the coupled oscillators (13) demonstrate complete synchronization in regimes of regular (at any positive coupling) and chaotic oscillations (at sufficiently large coupling).

Let us first consider the system of identical oscillators ($\Delta=0$). We choose $c=4.6$ which relates to a spiral chaotic attractor. The correspondent phase portraits and power spectrum are shown in Fig. 7(a). The power spectrum of the oscillations has a narrow peak at frequency $f_0=0.172$ and peaks at its harmonics kf_0, $k=2,3,4,\ldots$. At large coupling ($\gamma>0.14$), the system demonstrates complete chaotic synchronization. Decreasing coupling leads to bubbling of the attractor and a gradual transition to unsynchronized behavior. The correspondent changes in the phase portraits and in the coherence function are depicted in Fig. 8. The dependence of the synchronization value on the coupling is depicted in Fig. 9(a) (solid line). It can be qualitatively subdivided into four different parts.

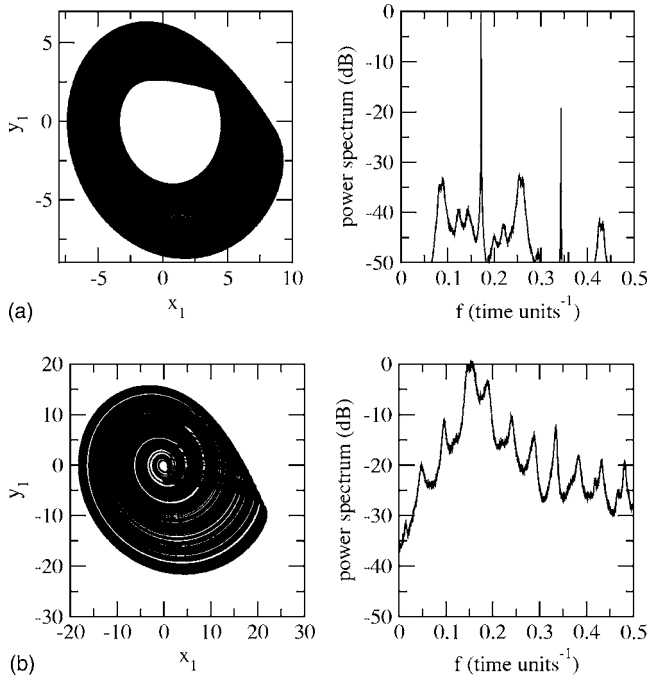

FIG. 7. A projection of phase portraits and the power spectrum of the Rossler oscillations in the regimes of spiral (a) and funnel (b) chaos.

(1) The region of strong full synchronization where $S \simeq 1$ for both noisy and noise-free systems. It corresponds to the values of the coupling $\gamma>0.17$.

(2) The region of weak full synchronization at $0.14<\gamma<0.17$, where complete synchronization exists only in the noise-free case. In this region, values of the synchronization index are different for the system without noise and with it. The coupling dependence of S for the system with additive noise of the amplitude $a=10^{-5}$ is depicted by the dashed line. This part of the curve is also shown in a larger scale in the box. The coherence function in the regime of full synchronization is evidently to be equal to 1 at all frequencies. According to the behavior of the coherence function regions (1) and (2) can be called a region of "total coherence."

(3) The region of slow monotonic decrease of the synchronization index from $S\simeq 1$ at $\gamma=0.14$ till $S\simeq 0.95$ at $\gamma=0.004$, which is associated with developing of the bubbling process [Figs. 8(b) and 8(c)]. The coherence function is less than 1, except at the basic frequency and its harmonics where it remains exactly equal to 1. We will call this region as a region of "basic coherence."

(4) The region of very small coupling $\gamma<0.004$ where synchronization quickly falls to zero at zero coupling. The coherence function is less than 1 for all frequencies (Figs. 8(d) and 8(e)]. This region can be called a region of "partial coherence" and the final point as "full incoherence."

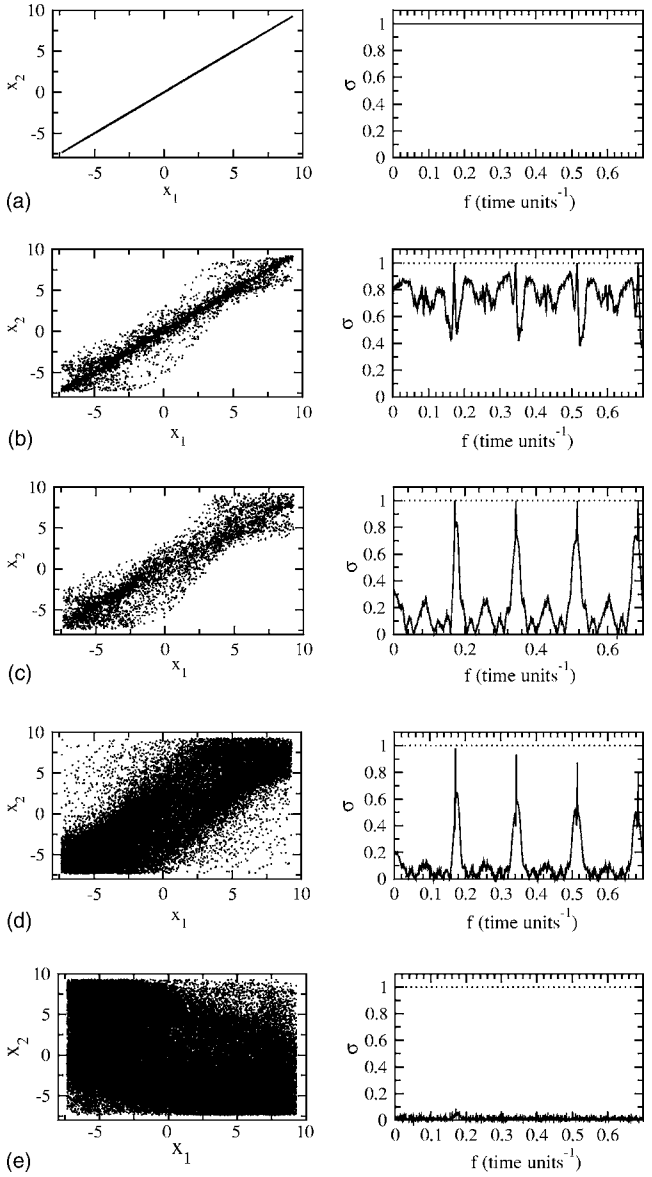

FIG. 8. Destruction of the complete chaotic synchronization in coupled Rossler oscillators in the regime of spiral chaos. A projection of the phase portrait and the coherence function for different values of the coupling: (a) $\gamma=0.16$; (b) $\gamma=0.1$; (c) $\gamma=0.01$; (d) $\gamma=0.004$; (e) $\gamma=0.0$.

Thus decreasing of the synchronization is characterized by two different stages: the slow stage with full coherence on the basic frequencies and the fast stage without such coherence. We supposed that the coherence at the basic frequencies can be connected with the instantaneous phases behavior. Hence, a different behavior of the synchronization index can be connected with the phenomenon of phase synchronization. To check this hypothesis, we considered a slightly mismatched system with $\Delta=0.01$. The behavior of the synchronization index for the mismatched oscillators is depicted by circles [Fig. 9(a)]. It is seen to be very similar to that of the identical systems and differs from it only in the regions of weak synchronization and of partial coherence. The last phenomenon begins at a stronger coupling ($\gamma \simeq 0.007$). To identify the phenomenon of phase synchronization, we investigate the behavior of the average periods in both oscillators as well as a time dependence of their instantaneous phases. The results of the calculations [Fig. 9(b) and Fig. 10] demonstrate an evident correlation between the loss of full coherence on the basic frequencies with the breaking of co-

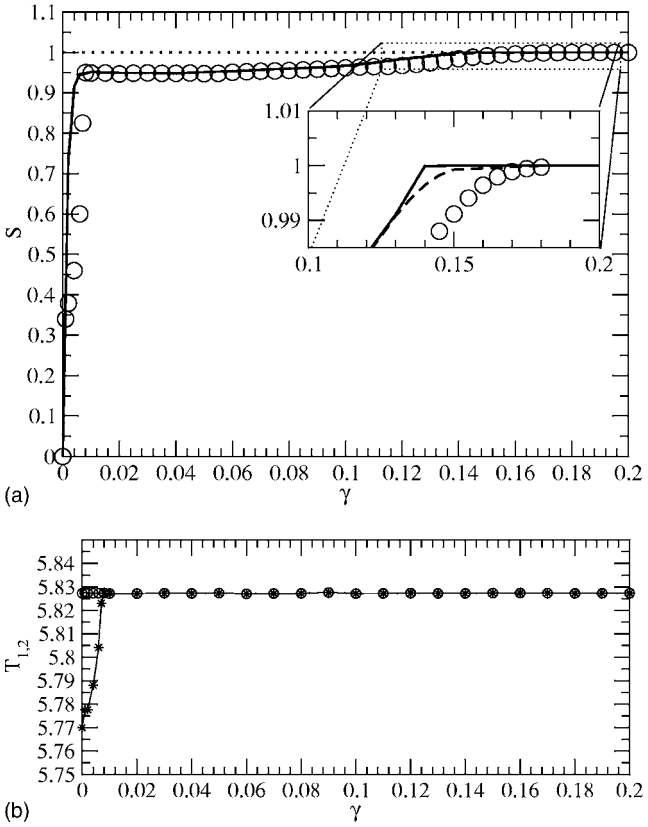

FIG. 9. (a) Coupling dependence of the synchronization index S for Rossler oscillators in the regime of spiral chaos: the solid line relates to the noise-free system, the dashed line relates to the system with additive noise with intensity $a=10^{-5}$ and symbols ○ mark the behavior for the mismatched oscillators at $\Delta=0.01$. (b) Coupling dependence of the average periods of oscillations in both subsystems. ○ : in the first oscillator; ∗ : in the second oscillator.

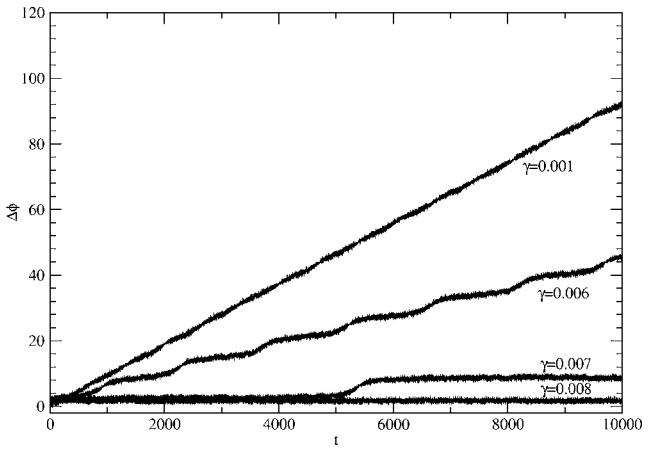

FIG. 10. Time dependence of differences of instantaneous phases for the Rossler oscillators with a parameter mismatch ($\Delta=0.01$) in the regime of spiral chaos.

incidence of the averaged periods. The "slow" part of the curve of the synchronization index takes place at the same interval of coupling where the average periods coincide, while its "fast" part takes place at a very small coupling, where the average periods are different. The synchronization of the average periods is a direct consequence of instantaneous phase locking that can be seen from Fig. 10 where we have built the time dependence of instantaneous phase differences at different coupling values: $\gamma=0.008$ that relates to the region of basic coherence, $\gamma=0.007$ and $\gamma=0.006$ related to the region of partial coherence and $\gamma=0.001$ relating to practically incoherent oscillations. Thus, from these dependencies we can conclude that perfect phase synchronization in the coupled Rossler oscillators takes place in the same region of coupling where the coherence function is equal to 1 at basic frequencies. When the full coherence at the basic frequencies becomes smaller than 1, the perfect phase synchronization is changed into an imperfect one ($\gamma=0.007$). This means that instantaneous phases remain locked during sufficiently long but finite time intervals, after which the phase difference "slips" to the next constant value. In the result, on the average the phase difference is slowly increased to infinity. With further coupling decreasing the coherence at the basic frequencies becomes smaller, that leads to a gradual transition from the imperfect phase synchronization to a totally unsynchronized behavior, when the intervals of phase locking becomes shorter and shorter and at a very small coupling disappears at all (see Fig. 10 at $\gamma=0.001$).

A similar behavior of the value S is observed for many-band attractors. In these cases the slow part of the curve becomes still slower and takes place until extremely small values of coupling, then it quickly falls to zero value at zero coupling. For example, in the case of a two-band attractor, the region of basic coherence lasts till values of coupling $\gamma \simeq 0.00002$. With an increase of the regularity of the chaos the shape of the dependence S on γ gradually tends to the threshold function: $S=1$ for $\gamma>0$, but $S=0$ for $\gamma=0$. The last dependence takes place for synchronization of periodic oscillations.

The instantaneous phases are known to be well defined when the chaotic attractor is quite "good," namely when its spectrum has a well distinguished peak on a frequency correspondent to some preferable time scale of oscillations. Therefore, oscillators with coherent chaos are typical models to investigate the phenomenon of chaotic phase synchronization. Does the phase synchronization exist in regimes of developed chaos? Attempts to find the answer to this question are still continued (see, for example Refs. [26–29]), but the problem remains under discussion. Nevertheless, the approach based on the coherence function remains valid in this case too and we can compare different stages of synchronous behavior in cases of highly developed chaos. For this purpose we consider the dynamics of the system (13) at $c=11.6$ that corresponds to a funnel attractor. A cross projection of its phase portrait and the power spectrum are depicted in Fig. 7(b). The power spectrum is sufficiently smooth but does not contain narrow peaks that evidence another character of chaos. In this regime the system (13) demonstrates the phenomenon of complete chaotic synchronization at sufficiently large coupling [Fig. 11(a)] and while the coupling decreases we can observe the same stages as for the spiral chaos: weak synchronization, bubbling behavior, and unsynchronized oscillations. The successive stages of the chaotic synchronization loss and accompanying changes of the coherence function are depicted in Figs. 11(b)–11(d). Though, according to phase portraits the synchronization destruction comes through the same stages as in the case of spiral chaos, the coherence function behaves differently (see the left column of Fig. 11). Contrary to the case of the spiral attractor, after the complete synchronization breaks, there are no frequencies of full coherence. The blowout bifurcation practically immediately leads to a simultaneous loss of coherence at all frequencies. Then, the coherence gradually decreases with a further decrease of γ. Consequently, the dependence

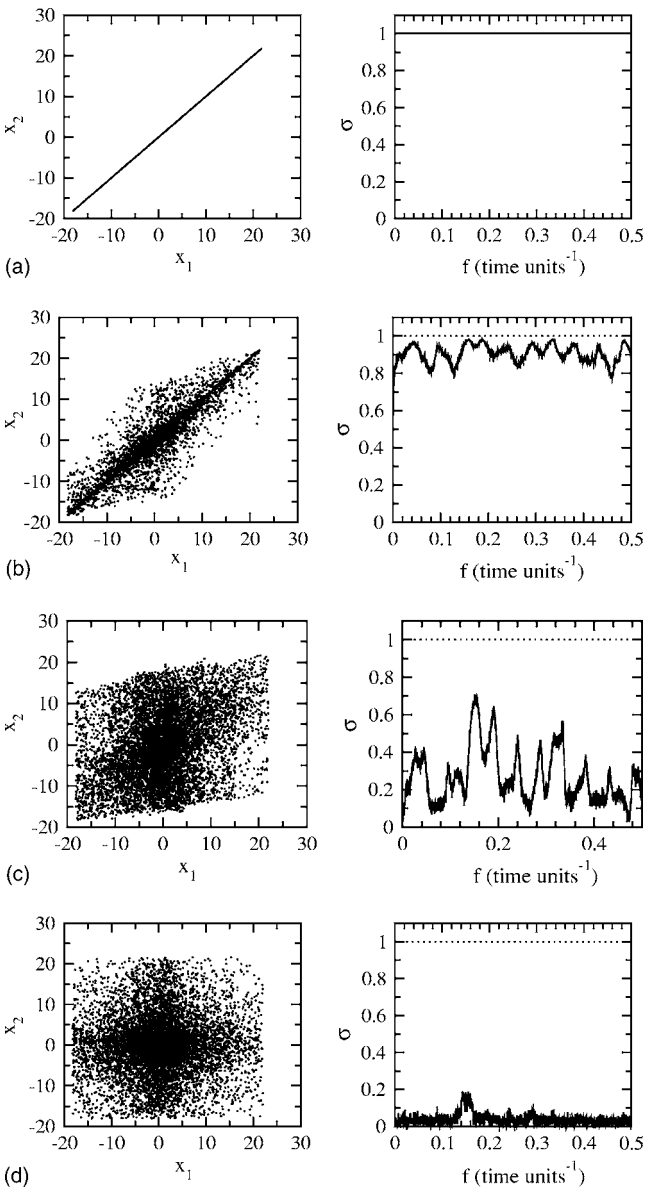

FIG. 11. Chaotic synchronization destruction with decreasing of coupling: a projection of the phase portrait and the coherence function. Parameter $c=11.6$ relates to the funnel chaotic attractor: (a) $\gamma=0.4$; (b) $\gamma=0.21$; (c) $\gamma=0.1$; (d) $\gamma=0.01$.

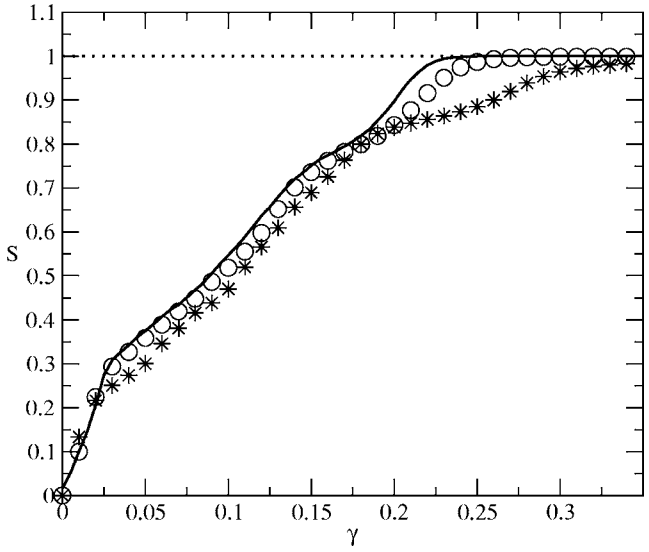

FIG. 12. Coupling dependence of the synchronization index for Rossler oscillators in the regime of funnel chaos: solid line ($\Delta=0$); circles ($\Delta=0.001$); stars ($\Delta=0.05$).

of the synchronization value S on the coupling does not demonstrate the mentioned above character: it monotonically decreases with an approximately constant speed to zero. The correspondent curve is depicted as a solid line in Fig. 12. A similar dependence remains for mismatched oscillations ("○" for $\Delta=0.01$ and "∗" for $\Delta=0.05$). Thus we see a qualitative difference between the synchronization breaking in cases of spiral and funnel attractors.

In the first case the loss of complete synchronization is followed by the phenomenon of phase synchronization, when the index of synchronization remains sufficiently large and slowly decreases with coupling. The coherence function demonstrates full coherence at basic frequencies. Then, the perfect phase synchronization is changed by an imperfect one, when the synchronization index quickly decreases with coupling to zero. The coherence function does not contain frequencies of full coherence.

In the last case we can not observe the phenomenon of phase synchronization. The coherence function has no frequencies of full coherence and the synchronization index behavior does not contain "slow" part.

V. CONCLUSION

We have shown that the coherence function is a very powerful tool for investigation of chaotic synchronization. The synchronization index (2) can be applied for measuring and diagnostics of different types of synchronous behavior: complete, generalized, lag, and phase synchronization. It is robust to small noise and distortions. The analysis carried out with the help of this characteristic has revealed a principal difference between synchronization in discrete maps and oscillators in regimes of coherent chaos. In the first case the index of synchronization tends to some nonzero value with a coupling decrease, while in the latter case it falls to zero at zero coupling. In the regime of spiral chaos in the coupled Rossler oscillators the phase synchronization phenomenon, which takes place after the complete synchronization breaks, can be diagnosed by the coherence function behavior: The instantaneous phases locking manifests itself in the full coherence on the basic frequencies of the power spectrum. In the regime of a funnel attractor the behavior of the coherence function is different. The full coherence exists only in the case of complete synchronization. After the complete synchronization breaks, the coherence becomes smaller than 1 at all frequencies.

Thus the average coherence can be used as another tool for the investigation of chaotic synchronization alongside with other synchronization measures. Our approach has the following main advantages, which are of importance for its applications.

It has a straightforward physical meaning which immediately follows from the traditional concept of synchronization of oscillations as frequency and phase entrainment.

Its calculation is based on well known and highly developed methods of spectral evaluation. It does not take any sophisticated algorithms and gives results which are stable to the choice of parameters of the numerical scheme. Thus the calculation of the synchronization index on formulas (2) or (3) represents a trivial task. On the contrary, a number of recent publications (see, for example, Ref. [30] and references there) evidences that correct calculations of entropy-like characteristics remains a sufficiently complex problem.

It gives the possibility to perform a selective analysis of synchronization on different time scales. This can be very useful when the dynamics of systems can be divided into "fast" and "slow" motions.

However, there are some open problems. A detailed comparison of the index (2) with the measures based on other principles is beyond the scope of the present investigation. Especially, the synchronization measures which are based on the information theory can provide indication of possible causal relationships between subsystems [31,32]. This can hardly be achieved in the framework of the proposed approach. Another open problem is a modification of this method for the analysis of larger ensembles of coupled oscillators.

ACKNOWLEDGMENTS

A.S. thanks the Ministry of Education and Science of Russian Federation and to the German Academic Exchange Service for the financial support of the research (Program "Mikhail Lomonosov"). V.A. thanks the Ministry of Education and Science of Russian Federation and CRDF for financial support (program BRHE, grant SR-006-X1).

[1] H. Fujisaka and T. Yamada, Prog. Theor. Phys. **69**, 32 (1983).
[2] V. S. Afraimovich, N. N. Verichev, and M. I. Rabinovich, Radiofiz. **29**, 1050 (1986).
[3] L. M. Pecora and T. L. Caroll, Phys. Rev. Lett. **64**, 821 (1990).
[4] V. S. Anishchenko, T. E. Vadivasova, D. E. Postnov, and M. A. Safonova, Int. J. Bifurcation Chaos Appl. Sci. Eng. **2**, 633 (1992).
[5] M. G. Rosenblum, A. S. Pikovsky, and J. Kurths, Phys. Rev. Lett. **76**, 1804 (1996).
[6] H. D. I. Abarbanel, N. F. Rulkov, and M. M. Sushchik, Phys. Rev. E **53**, 4528 (1996).
[7] M. G. Rosenblum, A. S. Pikovsky, and J. Kurths, Phys. Rev. Lett. **78**, 4193 (1997).
[8] R. Quian Quiroga, A. Kraskov, T. Kreuz, and P. Grassberger, Phys. Rev. E **65**, 041903 (2002).
[9] A. Shabunin, V. Demidov, V. Astakhov, and V. Anishchenko, Phys. Rev. E **65**, 056215 (2002).
[10] S. J. Schiff, P. So, and T. Chang, Phys. Rev. E **54**, 6708 (1996).
[11] J. Arnhold, P. Grassberger, K. Lehnertz, and C. E. Elger, Physica D **134**, 419 (1999).
[12] A. Schmitz, Phys. Rev. E **62**, 7508 (2000).
[13] M. A. Kramer, E. Edwards, M. Soltani, M. Berger, R. Knight, and A. J. Szeri, Phys. Rev. E **70**, 011914 (2004).
[14] M. C. Romano, M. Thiel, J. Kurths, and W. von Bloh, Phys. Lett. A **330**, 214 (2004).
[15] V. S. Anishchenko, V. V. Astakhov, V. V. Nikolaev, and A. V. Shabunin, J. Commun. Technol. Electron. **45**, 179 (2000).
[16] A. Shabunin, V. Astakhov, and V. Anishchenko, Int. J. Bifurcation Chaos Appl. Sci. Eng. **12**, 1895 (2002).
[17] S. L. Marple, *Digital Spectral Analysis with Applications* (Prentice-Hall, Inc., Englewood Cliffs, NJ, 1987).
[18] P. Ashvin, J. Buescu, and I. Stewart, Phys. Lett. A **193**, 126 (1994).
[19] P. Ashvin, J. Buescu, and I. Stewart, Nonlinearity **9**, 703 (1996).
[20] J. F. Heagy, T. L. Carroll, and L. M. Pecora, Phys. Rev. Lett. **73**, 3528 (1994).
[21] V. Astakhov, A. Shabunin, T. Kapitaniak, and V. Anishchenko, Phys. Rev. Lett. **79**, 1014 (1997).
[22] V. Astakhov, M. Hasler, T. Kapitaniak, A. Shabunin, and V. Anishchenko, Phys. Rev. E **58**, 5620 (1998).
[23] Y. L. Maistrenko, V. L. Maistrenko, and A. Popovich, Phys. Rev. E **57**, 2713 (1998).
[24] V. V. Demidov, "*Mechanisms of Synchronization Lost in UnidirectionallyCoupled Chaotic Systems*," in Proceedings of Scientific Conference: "Nonlinear Days in Saratov," Saratov, 2000, p. 60.
[25] C. Masoller and D. H. Zanette, Physica A **300**, 359 (2001).
[26] M. A. Zaks, E.-H. Park, M. G. Rosenblum, and J. Kurths, Phys. Rev. Lett. **82**, 4228 (1999).
[27] E.-H. Park, M. A. Zaks, and J. Kurths, Phys. Rev. E **60**, 6627 (1999).
[28] J. Y. Chen, K. W. Wong, and J. W. Shuai, Phys. Lett. A **285**, 312 (2001).
[29] G. V. Osipov, B. H. Hu, C. Zhou, M. V. Ivanchenko, and J. Kurths, Phys. Rev. Lett. **91**, 024101 (2003).
[30] A. Kraskov, H. Stogbauer, and P. Grassberger, Phys. Rev. E **69**, 066138 (2004).
[31] T. Schreiber, Phys. Rev. Lett. **85**, 461 (2000).
[32] R. Quian Quiroga, J. Arnhold, and P. Grassberger, Phys. Rev. E **61**, 5142 (2000).